Advance Publication Cover Page

Bulletin of the Chemical Society of Japan

Photoswitchable Turn-on Mode Fluorescent Diarylethenes: Strategies for Controlling the Switching Response

Masahiro Irie* and Masakazu Morimoto

Advance Publication on the web December 19, 2017
doi:10.1246/bcsj.20170365

Photoswitchable Turn-on Mode Fluorescent Diarylethenes: Strategies for Controlling the Switching Response

Masahiro Irie* and Masakazu Morimoto

Department of Chemistry and Research Center for Smart Molecules
Rikkyo University
Nishi-Ikebukuro 3-34-1, Toshima-ku, Tokyo, 171-8501, Japan

Abstract:
A new type of photoswitchable fluorescent diarylethenes, which have no fluorophore unit but emit strong fluorescence ($\Phi_f \sim 0.9$) in the closed-ring isomers, has been developed. They are sulfone derivatives of 1,2-bis(2-alkyl-4-methyl-5-phenyl-3-thienyl)perfluorocyclopentenes and 1,2-bis(2-alkyl-1-benzothiophen-3-yl)perfluorocyclopentenes. By chemical modifications of the structures their switching response was tuned to meet the requirements for super-resolution fluorescence microscopies. The water-soluble derivatives have been successfully applied to acquire super-resolution bioimages using a single-wavelength visible beam.

Fluorescence is the most convenient tool to detect small amounts of molecules.[1] Even single molecules can be detected using the fluorescence owing to remarkable progress of optical detection techniques.[2 - 4] Various types of highly fluorescent chromophores have been synthesized and widely applied in materials and life sciences, such as microanalysis and bioimaging.[5 - 9] Their application is expected to be further extended when an additional switching property is provided to the chromophores.[10] The changes in fluorescence spectra and/or intensity by external stimuli, such as chemicals, electrons (or holes) or photons, are ingeniously adopted for the analysis and the imaging. When the fluorescence is photoactivated or switched *on* and *off* upon photoirradiation, the fluorescence modulation offers the opportunities to monitor diffusion processes in real time,[11 – 13] store optical information in memory media,[14 - 20] and increase the resolution in imaging.[10, 20 - 23]

There are two types of fluorescence switching molecules, photoactivatable and photoswitchable ones. The photoactivatable molecules irreversibly switch from non-fluorescent to fluorescent states, while photoswitchable ones undergo reversible switching between fluorescent and non-fluorescent states. The reversibly photoswitchable molecules can be designed and constructed by integrating both photochromic and fluorescent chromophores in a molecule.[14 - 20] Based on this strategy numerous photoswitchable fluorescent molecules have been synthesized. Even limited to molecules having a photochromic diarylethene derivative as a photoswitching unit, a number of derivatives having a fluorescent unit, such as triphenyl imidazole,[24] anthracene,[14, 15, 25, 26] perylenebisimide,[16 – 19, 27] or indacene,[28] have been prepared. The molecules are initially fluorescent, while the fluorescence is quenched by an energy or an electron transfer mechanism when the diarylethene unit converts from the open- to the closed-ring isomer upon UV irradiation. The fluorescence switching from fluorescent to non-fluorescent states can be applied to optical memory media but is hardly applicable to super-resolution bioimaging, which visualizes and tracks microstructures and molecular events in cells.[29]

Recent progress of fluorescent microscopies has revolutionized the optical imaging, especially spatial resolution.[30, 31] The diffraction limit no longer restricts the spatial resolution in optical microscopy; it was overcome by using photoswitching of fluorescent probes between dark and emitting states. The super-resolution techniques are usually grouped into two categories, coordinate-targeted and coordinate-stochastic methods. In coordinate-targeted methods (stimulated emission depression (STED)[32 - 34] and reversible saturable (switchable) optical linear fluorescence transition (RESOLFT) microscopies[35, 36]), the position of the *on* and *off* states is determined by a doughnut-shaped pattern of light inducing a turn-on or a turn-off transition in the sample, except at the central position with vanishing intensity. In coordinate-stochastic super-resolution microscopies (photoactivated localization microscopy

(PALM)[37, 38] and stochastic optical reconstruction microscopy (STORM)[39, 40]), fluorescence *off–on* events take place molecules by molecules, with the molecules located at random positions. PALM and STORM are based on the technique to detect single fluorescent molecules.

The reversibly photoswitchable fluorescent molecules can be applied to both RESOLFT microscopy and PALM/STORM, while the irreversibly photoactivatable molecules can be used only for PALM/STORM. The application of turn-off mode photoswitchable fluorescent molecules to PALM/STORM is limited, because the fluorescence quenching, in many cases, is imperfect and the imaging technique requires a dark background to detect single fluorescent molecules. For the application, it is strongly desired to develop turn-on mode photoswitchable fluorescent molecules, which can efficiently and instantaneously activated upon photoirradiation.

Although several turn-on mode photoactivatable fluorophores, such as dihydrofuran,[41] coumarine,[42] fluorescein,[43] rhodamine[44] and anthracene,[45] have been reported, their photoactivation quantum yields are relatively low and the reactions are irreversible. Recently, a new type of turn-on mode photoswitchable fluorescent molecules have been developed. They are sulfone derivatives of 1,2-bis(2-alkyl-4-methyl-5-phenyl-3-thienyl)perfluorocyclopentenes[46] and 1,2-bis(2-alkyl-1-benzothiophen-3-yl)perfluorocyclopentenes.[47] Although they are initially non-luminous under excitation with visible light, they emit strong fluorescence upon irradiation with UV light.

In this account we describe how to improve the photochemical and photophysical properties of the sulfone derivatives by chemical modifications to meet the requirements for super-resolution fluorescence microscopies. New molecular photoswitches with improved and outstanding properties will surely contribute to the progress of super-resolution fluorescence bioimaging.

1. Photoswitchable highly fluorescent diarylethenes

Sulfone derivatives of 1,2-bis(2-alkyl-4-methyl-5-phenyl-3-thienyl)perfluorocyclopentenes. 1,2-Bis(2,4-dimethyl-5-phenyl-3-thienyl)perfluorocyclopentene (**1**) is one of typical photochromic diarylethenes.[48 - 50] The open-ring **1a** isomer converts to the closed-ring **1b** isomer upon irradiation with UV light. The colorless *n*-hexane solution containing **1a** (λ_{max} = 268 nm, $\varepsilon = 2.8 \times 10^4$ M^{-1} cm^{-1}) turns to blue due to the formation of **1b** (λ_{max} = 562 nm, $\varepsilon = 1.1 \times 10^4$ M^{-1} cm^{-1}). Upon irradiation with visible light (λ > 450 nm) **1b** returns back to **1a** and the blue color disappears. The cyclization and cycloreversion quantum yields were determined to be 0.45 and 0.018, respectively. Although **1** exhibits an excellent color change, both isomers are non-fluorescent.

During the course of study on the fatigue property of diarylethene derivatives Ahn and

co-workers[51 - 55] found that oxidation of sulfur atoms to sulfones is effective to provide a fluorescent property to the derivatives. Following up the research the synthesis of a dithienylperfluorocyclopentene derivative having thiophene 1,1-dioxide groups was examined.[52, 56] As expected the derivative, 1,2-bis(2,4-dimethyl-5-phenylthiophene-1,1-dioxide-3-yl)perfluorocyclopentene (**2**), switched to a fluorescent dye upon UV irradiation. Upon irradiation with UV light the open-ring **2a** isomer converted to the closed-ring **2b** isomer and the photogenerated **2b** emitted fluorescence under excitation with 423 nm light. The fluorescence quantum yield was, however, as low as 0.03 in 2-methylteterahydrofuran. Although **2** exhibits the turn-on mode fluorescence property, the low fluorescence quantum yield prevents its practical use. To improve the fluorescence performance chemical modifications were made and it was found that introduction of short alkyl chains at 2- and 2'-positions of the thiophene 1,1-dioxide groups is effective to increase the fluorescence quantum yield.[46]

Scheme 1 shows the structures of derivatives prepared. Figure 1 shows the absorption and fluorescence spectra of **3**-**6** in 1,4-dioxane. The 1,4-dioxane solutions of **3a**-**6a** are colorless and have no absorption in the visible-wavelength region, while upon irradiation with UV light **3a**-**6a** converted to **3b**-**6b** and the solutions turned yellow. The closed-ring **3b**-**6b** isomers emit green fluorescence around 530 nm upon excitation with 430 nm light. Subsequent irradiation with visible light (λ > 450 nm) caused the cycloreversion reactions from **3b**-**6b** to **3a**-**6a** and the absorption and fluorescence spectra decreased. Thus, **3**-**6** undergo cyclization/cycloreversion reactions and fluorescence switching upon alternate irradiation with UV and visible light.

[Scheme 1]

[Figure 1]

Table 1 summarizes photophysical and photochemical properties of diarylethenes **2**-**6** in 1,4-dioxane. Alkyl substitution at 2- and 2'-positions markedly affected the fluorescence quantum yield and the cycloreversion reaction. When methyl substituents were replaced with ethyl, *n*-propyl, isopropyl and isobutyl substituents, the fluorescence quantum yield increased dramatically from 0.07 to 0.42 – 0.50. The fluorescence quantum yield was significantly improved by replacing the methyl substituents with longer or branched alkyl ones. Photocyclization and photocycloreversion quantum yields are also shown in Table 1. The cyclization quantum yields of **2a**-**6a** are moderate and almost in the range of 0.1-0.2. The alkyl substituents scarcely affected the photocyclization reactivity. The cycloreversion quantum yields of **2b**-**5b** are in the order of 10^{-5}, which are much lower than the yield of non-oxidized diarylethene **1b** (0.018).[50] When sulfur atoms were oxidized to sulfones, the cycloreversion reaction was strongly suppressed. It is worth to note that the cycloreversion quantum yield of **6b**, which has isobutyl substituents at 2- and 2'-positions, increases to 2.1×10^{-3}, which is 81 times

larger than that of **5b**. Although the origin of the effect of isobutyl substitution is not clear at present, this result indicates that introduction of isobutyl substituents at the reactive carbons is useful to increase the cycloreversion quantum yield.

[Table 1]

Figure 2 shows the relationship between the quantum yields and the dielectric constants of the solvents. Methyl substituted derivative **2b** shows relatively high fluorescence quantum yield in non-polar *n*-hexane, while the yield dramatically decreases to 0.07 in 1,4-dioxane and further decreases to 0.02 in ethanol. In contrast, diarylethenes **3b**-**6b** keep relatively high yields even in ethanol. In ethanol the yields of ethyl and *n*-propyl substituted derivatives (**3b** and **4b**) are 0.18 and 0.19, respectively. The derivatives having branched alkyl substituents (**5b** and **6b**) show higher values (**5b**: 0.32, **6b**: 0.27). These results indicate that introduction of branched alkyl substituents into the reactive carbon atoms is effective to improve the fluorescent performance in polar solvents.

[Figure 2]

Sulfone derivatives of 1,2-bis(2-alkyl-6-aryl-1-benzothiophen-3-yl)perfluorocyclopentenes. 1,2-Bis(2-methyl-1-benzothiophen-3-yl)perfluoropentene (**7**) is also one of typical photochromic diarylethenes, which undergo thermally irreversible and fatigue resistant photochromic reactions.[48, 50, 57, 58] The open-ring **7a** isomer converts to the closed-ring **7b** isomer upon irradiation with UV light. The colorless *n*-hexane solution containing **7a** (λ_{max} = 258 nm, $\varepsilon = 1.5 \times 10^4$ M^{-1} cm^{-1}) turns red due to the formation of **7b** (λ_{max} = 516 nm, $\varepsilon = 1.0 \times 10^4$ M^{-1} cm^{-1}). Upon irradiation with visible light (λ > 450 nm) **7b** turns back to **7a** and the red color disappears. The cyclization and cycloreversion quantum yields were determined to be 0.31 and 0.29, respectively. In contrast to dithienylethene **1** both open- and closed-ring isomers of **7** exhibit weak fluorescence. The quantum yields of the open- and closed-ring isomers are reported to be 0.012 and ~0.0001, respectively.[53, 59]

Oxidation of the sulfur atoms to sulfones improved the fluorescent property. Figure 3 shows the absorption and fluorescence spectra of 1,2-bis(2-methyl-1-benzothiophen-1,1-dioxide-3-yl)perfluorocyclopentene (**8**) in ethyl acetate.[51] The absorption spectrum of the open-ring **8a** isomer is in the UV region and the ethyl acetate solution is colorless, while the closed-ring **8b** isomer generated by irradiation with UV light has absorption at 398 nm and the solution is pale yellow. The absorption band shows a significant hypsochromic shift in comparison with that of non-oxidized **7b**. Upon excitation with 400 nm light **8b** exhibits fluorescence. The fluorescence quantum yields of the open- and closed-ring isomers are reported to be 0.025 and 0.011, respectively.[53]

[Figure 3]

Although both non-oxidized derivative **7** and oxidized sulfone derivative **8** possess the turn-on mode fluorescence switching property, their fluorescence quantum yields are too low to be applied to super-resolution fluorescence microscopies. For the application it is required to improve the fluorescence performance: (i) increase in the absorption coefficient, (ii) bathochromic shift of the absorption and fluorescence spectra, and (iii) increase in the fluorescence quantum yield.

Just as examined in sulfone derivatives of 1,2-bisthienylethenes linear or branched alkyl chains were substituted at 2- and 2'-positions of the benzothiophene 1,1-oxide groups.[78, 60] Aryl substituents were also introduced at 6- and 6'-positions. Scheme 2 shows the structures of the modified sulfone derivatives. Both alkyl and aryl substituents markedly influenced the photochromic performance and the fluorescence property. Figure 4 shows the absorption and fluorescence spectra of **9** having methyl substituents at 2- and 2'-positions and **12** having *n*-butyl substituents in 1,4-dioxane. The open-ring **9a** and **12a** isomers have no absorption in the visible wavelength region (λ > 400 nm) and convert to the closed-ring **9b** and **12b** isomers having absorption in the visible wavelength region upon irradiation with UV (330 nm) light. The absorption maxima of **9a** and **12a** are observed at 296 nm and 298 nm, respectively, while those of **9b** and **12b** show the maxima at 443 nm and 456 nm, respectively. The absorption maxima of the closed-ring isomers of these aryl substituted derivatives showed a significant bathochromic shift in comparison with that of non-substituted derivative **8b**. In addition, the absorption coefficients increased two or three times. Both closed-ring isomers exhibited brilliant green fluorescence at around 540 nm. The fluorescence quantum yield was found to increase from 0.011 up to 0.89 in 1,4-dioxane by introducing *n*-propyl substituents at 2- and 2'-positions and phenyl substituents at 6- and 6'-positions.

[Scheme 2]

[Figure 4]

Table 2 summarizes photophysical and photochemical properties of the derivatives having various alkyl substituents. As can be seen from Table 2 the absorption maxima of the open-ring isomers are similar, but the absorption maxima of the closed-ring isomers show significant bathochromic shifts when substituents are altered from methyl to ethyl, *n*-propyl, *n*-butyl or isobutyl substituents.

[Table 2]

Solvent polarity dependence of the fluorescence quantum yields of **9b**-**13b** was examined as shown in Figure 5. The quantum yield of **9b** having methyl substituents dramatically decreases with increase in the solvent polarity, while the decrease is moderate for ethyl, *n*-propyl, *n*-butyl and isobutyl substituted derivatives **10b**-**13b**. The ethyl-substituted derivative **10b** keeps the quantum yield of 0.70 even in polar acetonitrile, while the methyl-substituted derivative **9b**

decreases the yield to 0.15. The different behavior can be explained as follows. In polar solvents, intermolecular interactions between the sulfone moieties and polar solvent molecules are considered to accelerate the non-radiative decay process. When bulky alkyl substituents are introduced at the connecting carbon atoms, they can defend the sulfone moieties from the attack of polar solvent molecules and suppress the non-radiative decay process. Thus, the derivatives having bulky alkyl substituents keep the relatively high fluorescence quantum yield even in polar solvents.

[Figure 5]

Figure 6 shows the absorption and fluorescence spectra of **14** in 1,4-dioxane.[48] Replacement of phenyl substituents at 6- and 6'-positions with thiophene rings shifts the absorption maximum of the closed-ring **14b** isomer to 506 nm ($\varepsilon = 5.8 \times 10^4$ M^{-1} cm^{-1}). The closed-ring isomer can be excited by irradiation with 532 nm light and emits brilliant orange fluorescence. The fluorescence quantum yield was measured to be 0.78 in 1,4-dioxane. **14b** is thermally as well as photochemically stable and hardly return back to the open-ring **14a** isomer by irradiation with visible light (the cycloreversion quantum yield < 10^{-5}). Figure 7 shows photographs of the fluorescence switching of 1,4-dioxane solutions containing **10** and **14** upon irradiation with 365 nm light under excitation with 488 nm (left-side solution containing **10**) and 532 nm light (right-side solution containing **14**). Before UV irradiation both solutions are non-luminous, while brilliant green and orange fluorescence emissions instantaneously appear upon UV irradiation. The emissions are attributable to the formation of fluorescent **10b** and **14b** isomers.

[Figure 6]

[Figure 7]

2. Control of Cycloreversion Quantum Yields

Coordinate-targeted super-resolution fluorescence microscopy, such as RESOLFT microscopy claims easy photoswitching of probe molecules from *on*-states to *off*-states upon irradiation with a doughnut-shaped low-power laser beam.[35, 36, 61] Therefore, it is required to develop photoswitchable fluorescent molecules with high switching-*off* (cycloreversion) efficiency. According to numerical simulations,[62] the resolution of images increases with increasing the switching-*off* quantum yield. However, if the quantum yield is too high, the irradiation that is required to probe the residual fluorescence will also deplete the fluorescence emission. To avoid the reduction in the fluorescence intensity during the probe phase, the quantum yield less than 10^{-2} is preferable. Taking into consideration of these factors, the optimal switching-*off* quantum yield is concluded to be in the order of 10^{-2} - 10^{-3}.

To obtain the desirable cycloreversion quantum yield for the RESOLFT microscopy, various substituents were introduced at 6- and 6'-positions of the sulfone derivatives of

1,2-bis(2-ethyl-1-benzothiophen-3-yl)perfluorocyclopentene.[63] The structures of the substituted derivatives are shown in Scheme 3. Although the cycloreversion quantum yield of unsubstituted sulfone derivative **15b** is 0.18,[47] introduction of phenyl substituents at 6- and 6'-positions, such as **10b**, decreases the yield to 5.9×10^{-4}. This result suggests that the cycloreversion quantum yield can be controlled by changing the aryl substituents, which affect the π-conjugation length and the coplanarity of the closed-ring isomers. In other words, the dihedral angle between the phenyl ring at 6-position (or 6'-position) and the oxidized benzothiophene is considered to influence the cycloreversion quantum yield.

[Scheme 3]

The absorption maxima of the open-ring isomers **15a**, **16a**, **17a** and **18a** were observed at 275 nm and 310 nm (**15a**), 293 nm and 328 nm (**16a**), 289 nm and 326 nm (**17a**), and 285 nm and 320 nm (**18a**), while those of the closed-ring isomers **15b**, **16b**, **17b**, and **18b** were observed at 414 nm, 445 nm, 441 nm, and 430 nm, respectively. The absorption maxima of the closed-ring isomers having *ortho*-substituted phenyl rings, **16b**, **17b**, and **18b**, showed a small but significant hypsochromic shift in comparison with that of **10b** (456 nm). The fluorescence quantum yields of **10b**, **16b**, **17b**, and **18b** were determined to be 0.87, 0.79, 0.84 and 0.79 in 1,4-dioxane, respectively. The yields are very similar and the *ortho*-substitution scarcely affects the fluorescence process.

Table 3 shows the cyclization and cycloreversion quantum yields of the derivatives having *ortho*-substituted phenyl rings. As shown in Tables 2 and 3, the cyclization quantum yields of the four derivatives, **10a**, **16a**, **17a**, and **18a**, are similar each other. On the other hand, the cycloreversion quantum yields are strongly dependent on the *ortho*-substitution. As described the previous section, the yield of **10b** is as low as 5.9×10^{-4}, while the yield increases to 2.8×10^{-3} (**16b**), 3.2×10^{-3} (**17b**), and 1.8×10^{-2} (**18b**) by introducing fluorine or methyl group(s) at *ortho*-position(s) of the phenyl rings. By replacing *ortho*-hydrogen with fluorine the yield increased by 5 times. The introduction of *ortho*-dimethyl substituents increased the yield by as large as 30 times. *Ortho*-substitution is very effective to increase the cycloreversion quantum yield to $10^{-2} - 10^{-3}$.

[Table 3]

Ortho-substitution is considered to decrease the coplanarity of the closed-ring isomers. Table 3 also shows the dihedral angles between the phenyl rings and the oxidized benzothiophene, which were measured by X-ray crystallographic analysis. When *ortho*-hydrogen is replaced with fluorine atom, such as **16b**, the dihedral angle increases from 30.2° to 35.9°. It further increases to 61.0° by introducing a methyl group. The dihedral angle of the derivative having *ortho*-dimethyl substituted phenyl ring is as large as 65.7°. The increase in the dihedral angle loses the coplanarity of the closed-ring isomer and decreases the extension of

π-conjugation length, resulting in the hypsochromic shift of the absorption spectrum and the increase in the cycloreversion quantum yield.

Figure 8 shows the correlation between absorption maxima of the closed-ring isomers and cyclization/cycloreversion quantum yields in less polar 1,4-dioxane and polar ethanol. Fluorescence quantum yields of the closed-ring isomers are also shown. Although the shift of the absorption maxima of the closed-ring isomers by *ortho*-substitutions scarcely affects the fluorescence quantum yields as well as cyclization quantum yields, it strongly increases the cycloreversion quantum yields by as large as 30 times. The photogenerated closed-ring isomers, **16b**, **17b**, and **18b**, exhibit brilliant green fluorescence with quantum yields higher than 0.79 and their cyclization quantum yields are higher than 0.58 in 1,4-dioxane. In addition, the cycloreversion quantum yields are in the range of $2.8 \times 10^{-3} - 1.8 \times 10^{-2}$. These compounds fulfill the necessary requirements for RESOLFT super-resolution microscopy.

[Figure 8]

Another strategy to increase the cycloreversion quantum yield is to introduce isobutyl substituents at reactive carbon atoms. As shown in Tables 1 and 2, the cyclization quantum yields of **6b** and **13b** having isobutyl substituents at 2- and 2'-positions of thiophene 1,1-dioxide or benzothiophene 1,1-dioxide are larger than the values of the derivative having ethyl substituents. The yields of **6b** and **13b** are more than one order of magnitude (19 – 55 times) larger than those of **3b** and **10b**. The cycloreversion quantum yields of these derivatives in the range of $10^{-2} - 10^{-3}$ are favorable for the application to RESOLFT microscopy.

3. Reversible Fluorescence Photoswitching by Irradiation with Single-Wavelength Visible Light [64]

As described in Introduction, localization super-resolution fluorescence microscopies, such as PALM and STORM, are based on single-molecule fluorescence detection. The large majority of probe molecules must be in the *off* states, except for a very sparse population that is in the *on* states. Both techniques require a dark background to detect single fluorescent molecules and need to turn *on* and *off* independently the emission of fluorophores positioned within the same diffraction limit. By adjusting the irradiation conditions on intensities of photoactivation as well as photobleaching only a sparse population of probe molecules is maintained in the emissive state during the image reconstruction sequence. Each localized probe at the single-molecular level is visualized in the form of a diffraction pattern and the center of the pattern can be approximated as the center of the molecule. The coordinate of each localized probe can then be stored and accumulated. This sequence of events, activation, localization and bleaching, is reiterated multiple times, until enough coordinates become available to reconstruct a complete image of the sample.

The diarylethenes so far synthesized, except several specially designed derivatives,[65 - 67] cannot be activated with visible light (> 400 nm). The visible light responsive property is favorable for the application to biological systems. During the course of study of photoswitchable diarylethenes we have discovered unprecedented photoreactions upon irradiation with single-wavelength visible light. Upon irradiation with the visible light both cyclization and cycloreversion reactions simultaneously take place and a very sparse population of molecules is reversibly activated to *on* states.

Upon irradiation with UV light (365 nm light) the open-ring **10a** isomers readily converted to the closed-ring **10b** isomers, which have absorption at 456 nm and give fluorescence at around 550 nm under excitation with 450 nm light. The photogenerated **10b** isomers were bleached upon irradiation with 450 nm light and reverted back to the open-ring **10a** isomers. Although both absorption and fluorescence spectra considerably decreased, noticeable intensity of fluorescence ascribed to **10b** remained even after prolonged irradiation with 450 nm light. **10a** has no apparent absorption at 450 nm. This means that all closed **10b** isomers are expected to completely revert back to the open-ring **10a** isomers by irradiation with 450 nm light. But, a small amount of **10b** survived. This result indicates that 450 nm light induces the cyclization reaction of **10a** in addition to the cycloreversion reaction.

We assumed that the reversible photoisomerizations are induced by irradiation with single-wavelength (λ) light.

$$\text{Open-ring isomer } \mathbf{10a} \underset{\lambda}{\overset{\lambda}{\rightleftharpoons}} \text{Closed-ring isomer } \mathbf{10b} \tag{1}$$

$$\frac{\mathrm{d}C_\mathrm{B}}{\mathrm{d}t} = (\Phi_{\mathrm{AB}}\varepsilon_\mathrm{A}C_\mathrm{A} - \Phi_{\mathrm{BA}}\varepsilon_\mathrm{B}C_\mathrm{B})F \tag{2}$$

$$F = \frac{1-e^{-(\varepsilon_\mathrm{A}C_\mathrm{A}+\varepsilon_\mathrm{B}C_\mathrm{B})d}}{\varepsilon_\mathrm{A}C_\mathrm{A}+\varepsilon_\mathrm{B}C_\mathrm{B}} \times \frac{10^3 I_0}{d}$$

where Φ_{AB}, Φ_{BA}, ε_A, ε_B, C_A, C_B, d, and I_0 are the cyclization quantum yield, the cycloreversion quantum yield, the absorption coefficient of **10a** at λ, the absorption coefficient of **10b** at λ, the concentration of **10a** (mol/L), the concentration of **1b** (mol/L), the cell length (cm), and the light intensity (einstein/cm^2·s), respectively. When $\varepsilon_\mathrm{A}C_\mathrm{A} + \varepsilon_\mathrm{B}C_\mathrm{B} << 1$, the formation of the closed-ring isomers is expressed as follows, where C_O is the total concentration of **10a** and **10b**.

$$C_\mathrm{B} = \frac{\Phi_{\mathrm{AB}}\varepsilon_\mathrm{A}}{\Phi_{\mathrm{AB}}\varepsilon_\mathrm{A}+\Phi_{\mathrm{BA}}\varepsilon_\mathrm{B}} C_\mathrm{O}\left(1 - e^{-(\Phi_{\mathrm{AB}}\varepsilon_\mathrm{A}+\Phi_{\mathrm{BA}}\varepsilon_\mathrm{B})\times 10^3 I_0 t}\right) \tag{3}$$

In the photostationary state,

$$\frac{C_\mathrm{B}}{C_\mathrm{0}} = \frac{\Phi_{\mathrm{AB}}\varepsilon_\mathrm{A}}{\Phi_{\mathrm{AB}}\varepsilon_\mathrm{A}+\Phi_{\mathrm{BA}}\varepsilon_\mathrm{B}} \tag{4}$$

Figure 9 shows the formation of **10b** from pure **10a** in *n*-hexane and CCl_4 upon irradiation

with 450 nm light. To detect a very small amount of **10b**, less than 10^{-7} M, fluorescence was used to measure the concentration. The formation curves were analyzed according to eq. (3). It is possible to determine the very weak absorption coefficients of **10a** at 450 nm from the concentration ratios of **10a** and **10b** in the photostationary state from eq. (4). Based on numerical simulations of the formation process of **10b** from **10a** the absorption coefficients at 450 nm in *n*-hexane and CCl_4 were estimated to be 0.084 M^{-1} cm^{-1} and 0.19 M^{-1} cm^{-1}, respectively. Although the absorption coefficients were very low, the formation of **10b** was clearly observed upon irradiation with 450 nm light. This is attributed to very low cycloreversion quantum yields of **10b** in *n*-hexane and CCl_4.

[Figure 9]

According to Wondrazek *et al.*[68] and Kinoshita *et al.*[69] the absorption spectra (or the emission excitation spectra) of fluorescent dyes, such as coumarin 7 and rhodamine 6G, show an exponential frequency dependence in the off-resonance region of the absorption tails at room temperature. The tails have been reported to obey the Urbach rule known in the absorption spectra of solid materials, as expressed by the following formula.[68 - 72]

$$\varepsilon(E) \propto \varepsilon(E_{00})\exp\left[-\frac{\sigma(E_{00}-E)}{k_{\mathrm{B}}T}\right] \qquad (5)$$

where ε, k_{B} , T, and σ are the absorption coefficient, the Boltzmann constant, the absolute temperature of the sample and the steepness parameter, respectively.

The absorption coefficients estimated from eq. (4) were plotted in Figure 10 along with the absorption tails of the open-ring **10a** isomer. As can be seen in Figure 10 the coefficients obey the exponential frequency dependence at the wavelengths longer than ~ 415 nm (~ 24000 cm^{-1}). The exponential frequency dependence indicates that the photoreactions with the visible light in the far-resonance region of the absorption edge are caused by the absorption of hot bands or Urbach tails. The open-ring **10a** isomers in the vibrationally excited states undergo optical transition into electronically excited states by absorbing the very weak hot bands and the cyclization reaction from **10a** to **10b** takes place. The reversible fluorescence photoswitching with single-wavelength visible light is advantageously applicable to super-resolution microscopies, as shown in the next section.

[Figure 10]

4. Application to Super-resolution Bioimaging [73 - 76]

As already being discussed in the previous sections, properly designed sulfone derivatives of bisthienylethenes and bisbenzothienylethenes fulfill the requirements for the application to super-resolution fluorescence microscopies. For the application to bioimaging another indispensable property is water solubility. Several approaches to provide water solubility to

diarylethenes have been reported.[77] In order to give both the water solubility and bioconjugation ability we introduced several carboxylic acid groups to the fluorescent diarylethenes. The presence of eight caroboxylates provided a fairly good solubility at pH > 5 and inhibited aggregation even after photocyclization. One of the carboxylates can be conveniently transformed into any reactive group for bioconjugation. Remarkably, the bioconjugates retain the photoswitching and fluorescent properties of the derivatives. The caroboxylated diarylethene **19** was applied to RESOLFT bioimaging.

To demonstrate the applicability of **19** for RESOLFT microscopy, fixed immunolabeled Vero cells were imaged using a modified IC RESOLFT QUAD Scanning microscope (Abberior Instruments, Göttingen). The imaging was performed by applying the following pulse sequence: switching the diarylethenes to their closed-ring isomers with 355 nm light (130 W cm^{-2}) for 50 μs, 200 μs delay, application of the doughnut-shaped 488 nm beam (36 kW cm^{-2}) for 1.2 ms to switch the diarylethenes in the periphery of the focal spot to their non-fluorescent open-ring isomers. Finally, the remaining area with the fluorescent isomers was probed for 80 μs with a Gaussian shaped 488 nm light beam (9.7 kW cm^{-2}). The confocal image was obtained by the same pulse sequence without the off-switching. Using this imaging scheme, it was possible to acquire RESOLFT images with a resolution of 74 nm FWHM (full width at half minimum) and confocal images of 175 nm FWHM. Figure 11 shows the RESOLFT and confocal images.

[Figure 11]

The success of the use of the diarylethene for RESOLFT is attributed to the relatively large cycloreversion quantum yield. The yield of **19b** was measured to be $2.0 \times 10^{-3} \pm 3 \times 10^{-4}$. **19b** was switched off in 1.5 ms. The resolution achieved in RESOLFT is limited mainly by the photobleaching rate and not by the residual fluorescence after *off*-switching. RESOLFT microscopy requires the cycloreversion quantum yield in the order of $10^{-2} – 10^{-3}$.

On the contrary, coordinate-stochastic super-resolution fluorescence microscopies, such as PALM and STORM, require a low cycloreversion quantum yield, because the resolution of these techniques depends on the localization process. Two important requirements for the probes are (i) a high number of photons detected during the *on* state to ensure a high localization accuracy, and (ii) the possibility to achieve a high [*off*]/[*on*] ratio to allow for a high labeling density. The second requirement is inherent to diarylethenes, because a complete conversion to open-ring isomers is achieved when the irradiation wavelength is properly selected to avoid excitation of hot bands or Urbach tails. The first requirement is dependent on both the ratio of emission efficiency (Φ_f) and the cycloreversion quantum yield (Φ_{BA}). **19b** used in the above RESOLFT microscopy presents $\Phi_f/\Phi_{BA} < 300$. This means that only 30 photons are expected to be detected during the *on* state in average, because a photon collection efficiency is around 10%.

To increase the localization accuracy, it is required to increase Φ_f/Φ_{BA} one order of magnitude. The preferable cycloreversion quantum yield is in the order of 10^{-4} or less. A sulfone derivative **20** having methoxy substituents and eight carboxylates in both sides was prepared and used for STORM. The cycloreversion and the fluorescence yields of **20b** were measured to be 1.8×10^{-4} and 0.45, respectively. Φ_f/Φ_{BA} increased to 2500.

The standard labeling protocol provided a reproducible control of the degree of labeling. The obtained bioconjugate was stable and showed no precipitation or aggregation after several months. The diarylethene retained the photoswitching ability even after bioconjugation with secondary antibodies and presented no reduction in the emission efficiency of the closed-ring isomer. Figure 12 shows the demonstration of wide-field STORM images. Photoactivation was carried out with 405 or 375 nm laser. Remarkably, it was possible to acquire up to - 200000 frames before any additional photoactivation with UV light. In other words, the *on* and *off* fluorescence switching of a sparse population of probe molecules can be attained by irradiation with only 488 nm laser. This imaging technique, which uses a single-wavelength visible beam without harmful UV light, is favorable for the application to biological systems. As described in the previous section, the activation in the absence of UV light is ascribed to the optical transition induced by the absorption of very weak hot bands or Urbach tails. Images acquired without and with UV photoactivation laser (375 nm) were identical within experimental error, as shown in Figure 12(b).

[Figure 12]

Here, super-resolution fluorescence imaging using photoswitchable fluorescent diarylethenes was demonstrated. By properly tuning the structures the derivatives were successfully applied to RESOLFT microscopy and STORM.

5. Summary and Future Prospect

A new type of turn-on mode fluorescent diarylethenes, which have no fluorophore unit but emit strong fluorescence ($\Phi_f \sim 0.9$) in the closed-ring isomers, has been synthesized and successfully applied to super-resolution fluorescence imaging, such as RESOLFT microscopy and PALM/STORM. Oxidation of sulfur atoms of 1,2-bis(2-alkyl-4-methyl-5-phenyl-3-thienyl)perfluorocyclopentenes and 1,2-bis(2-alkyl-1-benzothiophen-3-yl)perfluorocyclopentenes was effective to provide a highly fluorescent property to the closed-ring isomers. By chemical modifications of the structures the physical and chemical properties of the diarylethenes were tuned to meet the requirements for the microcopies. RESOLFT microcopy requires the cycloreversion quantum yield in the order of $10^{-2} – 10^{-3}$, while the yield in the order of 10^{-4} or less is claimed in PALM/STORM imaging. The cycloreversion as well as fluorescence quantum yields were optimized by introducing

appropriate alkyl and aryl substituents to thiophene 1,1-dioxide and benzothiophene 1,1-dioxide groups. The water-soluble derivatives have been applied to acquire super-resolution bioimages using a single-wavelength visible beam.

The super-resolution microscopies using photoswitchable diarylethenes can be applied not only to biological systems but also to materials science. It is capable of resolving apolar nano-structures in cylindrical micelles formed by amphiphilic block copolymers by using super-resolution PALM.[74] The progress of super-resolution microscopy technique is continuing. Recently, Hell and co-workers[78] reported a new nanometer-resolution imaging method named MINFLUX. The method can image individual molecules separated by just 1 nm. The present photoswitchable diarylethenes have a potential to be used in the MINFLUX microscopy.

Acknowledgments

This work was supported by MEXT-Supported Program for Scientific Research Foundation at Private Universities. We are grateful to Prof. K.-H. Ahn (Kyung Hee University) for early discussion on the synthesis of sulfone derivatives. We also wish to express our thanks to Prof. S. W. Hell and Dr. V. N. Belov (Max Planck Institute for Biophysical Chemistry) for their guidance and collaboration to use the compounds for super-resolution fluorescence microscopies.

References

1. J. R. Lakowicz, *Principles of fluorescent spectroscopy*, *3rd ed*. Springer, New York, **2010.**
2. W. E. Moerner, L. Kador, *Phys. Rev. Lett*. **1989**, *62*, 2535.
3. E. Betzig, R. J. Chichester, *Science* **1993**, *262*, 1422.
4. R. Rigler, M. Oritt, T. Basché, *Single molecule spectroscopy. Nobel conference lectures* Springer-Verlag, Berlin, **2001**.
5. S. W. Thomas, G. D. Joly, T. M. Swager, *Chem. Rev*. **2007**, *107*, 1339.
6. X. Chen, T. Pradhan, F. Wang, J. S. Kim, J. Yoon, *Chem. Rev*. **2012**, *112*, 1910.
7. X. F. Wang, B. Herman, *Fluorescence Imaging Spectroscopy and Microscopy* John Wiley & Sons, New York, **1996**.
8. R. Ando, H. Mizuno, A. Miyawaki, *Science* **2004**, *306*, 1370.
9. A. S. Stender, K. Marchuk, C. Liu, S. Sander, M. W. Meyer, E. A. Smith, B. Neupane, G. Wang, J. Li, J-. X. Cheng, B. Huang, N. Fang, *Chem. Rev*. **2013**, *113*, 2469.
10. F. M. Raymo, *Phys. Chem. Chem. Phys*. **2013**, *15*, 14840.
11. T. J. Johnson, D. Ross, M. Gaitan, L. E. Locascio, *Anal. Chem*. **2001**, *73*, 3656.
12. J. Patrick, D. T. Chiu, *Anal. Chem*. **2003**, *75*, 1387.
13. G. Zheng, Y-M. Guo, W-H. Li, *J. Am. Chem. Soc*. **2007**, *129*, 10616.
14. M. Irie, T. Fukaminato, T. Sasaki, N. Tamai, T. Kawai, *Nature* **2002**, *420*, 759.
15. T. Fukaminato, T. Sasaki, T. Kawai, N. Tamai, M. Irie, *J. Am. Chem. Soc.* **2004**, *126*, 14843.
16. T. Fukaminato, T. Umemoto, Y. Iwata, S. Yokojima, M. Yoneyama, S. Nakamura, M. Irie, *J. Am. Chem. Soc.* **2007**, *129*, 5932.
17. T. Fukaminato, T. Doi, N. Tamaoki, K. Okuno, Y. Ishibashi, H. Miyasaka, M. Irie, *J. Am. Chem. Soc.* **2011**, *133*, 4984.
18. M. Berberich, A.-M. Krause, M. Orlandi, F. Scandola, F. Würthner, *Angew. Chem. Int. Ed.* **2008**, *47*, 6616.
19. M. Berberich, M. Natali, O. Spenst, C. Chiorboli, F. Scandola, F. Würthner, *Chem. Eur. J.* **2012**, *18*, 13651.
20. T. Fukaminato, *J. Photochem. Photobiol. C.* **2011**, *12*, 177.
21. M. Heilmann, P. Dedecker, J. Hofkens, M. Sauer, *Laser Photon. Rev*. **2009**, *3*, 180.
22. A. Fürstenberg, M. Heilemann, *Phys. Chem. Chem. Phys.* **2013**, *15*, 14919.
23. J. Kwon, J. Hwang, J. Park, G. R. Han, K. Y. Han, S. K. Kim, *Sci. Rep*. **2014**, *5*, 17804.
24. K. Yagi, C. F. Soong, M. Irie M, *J. Org. Chem.,* **2001**, *66*, 5419.
25. A. de Meijere, L. Zhao, V. N. Belov, M. L. Bossi, M. Noltemeyer, S. W. Hell, *Chem. Eur. J.* **2007**, *13*, 2503.
26. H. Ohara, M. Morimoto, M. Irie, *Photochem. Photobiol. Sci.* **2010**, *9*, 1079.

27. M. Pärs, C. C. Hofmann, K. Willinger, P. Bauer, M. Thelakkat, J. Köhler, *Angew. Chem. Int. Ed.* **2011**, *50*, 11405.
28. T. A. Golovkova, D. V. Kozlov, D. C. Neckers, *J. Org. Chem.* **2005**, *70*, 5545.
29. P. Sengupta, S. B. van Engelenburg, J. Lippincott-Schwartz, *Chem. Rev*. **2014**, *114*, 3189.
30. S. W. Hell, *Science* **2007**, *316*, 1153.
31. S. W. Hell, *Nat. Methods* **2009**, *6*, 24.
32. S. W. Hell, J. Wichmann, *J. Opt. Lett*. **1994**, *19*, 780.
33. V. Westphal, S. O. Rizzoli, M. A. Lauterbach, D. Kamin, R. Jahn, S. W. Hell, *Science* **2008**, *320*, 246.
34. S. Berning, K. I. Willing, H. Steffens, P. Dibai, S. W. Hell, *Science* **2012**, *335*, 551.
35. S. W. Hell, S. Jakobs, L. Kastrup, *Appl. Phys. A* **2003**, *77*, 859.
36. M. Hoffmann, C. Eggeling, S. Jakobs, S. W. Hell, *Proc. Nat. Acad. Sci. USA* **2005**, *102*, 17565.
37. E. Betzig, G. H. Patterson, R. Sougrat, O. W. Lindwasser, S. Olenych, J. S. Bonifacino, M. W. Davidson, J. Lippincott-Schwartz, H. F. Hess, *Science* **2006**, *313*, 1642.
38. S. T. Hess, T. P. K. Girirajan, M. D. Mason, *Biophys. J.* **2006**, *91*, 4258.
39. M. J. Rust, M. Bates, X. Zhuang, *Nat. Methods* **2006**, *3*, 793.
40. M. Bates, B. Huang, G. T. Dempsey, X. W. Zhuang, *Science* **2007**, *317*, 1749.
41. S. J. Lord, N. R. Conley, H. D. Lee, R. Samuel, N. Liu, R. J. Twieg, W. E. Moerner, *J. Am. Chem. Soc.* **2008**, *130*, 9204.
42. E. Deniz, M. Tomasulo, J. Cusido, I. Yildiz, M. Petriella, M. L. Bossi, S. Sortino, F. M. Raymo, *J. Phys. Chem. C.* **2012**, *116*, 6058.
43. T. Kobayashi, Y. Urano, M. Kamiya, T. Ueno, H. Kojima, T. Nagano, *J. Am. Chem. Soc.* **2007**, *129*, 6696.
44. J. Fölling, V. N. Belov, R. Kunetsky, R. Medda, A. Schönle, A. Egner, C. Eggeling, M. L. Bossi, S. W. Hell, *Angew, Chem. Int. Ed*. **2007**, *46*, 6266.
45. E. R. Thapaliya, B. Captain, F. M. Raymo, *J. Org. Chem.* **2014**, *79*, 3973.
46. M. Morimoto, T. Sumi, M. Irie, *Materials* **2017**, *10*, 1021.
47. K. Uno, H. Niikura, M. Morimoto, Y. Ishibashi, H. Miyasaka, M. Irie, *J. Am. Chem. Soc.* **2011**, *133*, 13558.
48. M. Irie, T. Fukaminato, K. Matsuda, S. Kobatake, *Chem. Rev*. **2014**, *114*, 12174.
49. M. Irie, K. Sakemura, M. Okinaka, K. Uchida, *J. Org. Chem*. **1995**, 60, 8305
50. T. Sumi, Y. Takagi, A. Yagi, M. Morimoto, M. Irie, *Chem. Commun*. **2014**, *50*, 3928.
51. Y-C. Jeong, S. I. Yang, K-h. Ahn, E. Kim, *Chem. Commun*. **2005**, 2503.
52. Y-C. Jeong, E. Kim, K-H. Ahn, S. I. Yang, *Bull. Korean Chem. Soc*. **2005**, *26*, 1675.
53. Y-C. Jeong, S. I. Yang, E. Kim, K-H. Ahn, *Tetrahedron* **2006**, *62*, 5855.

54. Y-C. Jeong, D. G. Park, E. Kim, K-H. Ahn, S. I. Yang, *Chem. Commun*. **2006**, 1881.
55. Y-C. Jeong, D. G. Park, I. S. Lee, S. I. Yang, K-H. Ahn, *J. Mater. Chem*. **2009**, *19*, 97.
56. M. Taguchi, T. Nakagawa, T. Nakashima, T. Kawai, *J. Mater. Chem*. **2011**, *21*, 17425.
57. M. Hanazawa, R. Sumiya, Y. Horikawa, M. Irie, *J. Chem. Soc., Chem. Commun*. **1992**, 206.
58. K. Uchida, E. Tsuchida, Y. Aoi, S. Nakamura, M. Irie, *Chem. Lett.* **1999**, *28*, 63.
59. S. Shim, T. Joo, S. C. Bae, k. S. Kim, E. Kim, *J. Phys. Chem. A* **2003**, *107*, 8106.
60. Y. Takagi, T. Kunishi, T. Katayama, Y. Ishibashi, H. Miayasaka, M. Morimoto, M. Irie, *Photochem. Photobiol. Sci.* **2012**, *11*, 1661.
61. T. Grotjohann, I. Testa, M. Leutenegger, H. Bock, N. T. Urban, F. Lavoie-Cardinal, K. I. Willig, C. Eggelling, S. Jakobs, S. W. Hell, *Nature* **2011**, *478*, 204.
62. P. Dedecker, J-i Hotta, C. Flors, M. Sliwa, H. Uji-i, M. B. J. Roeffaers, R. Ando, H. Mizuno, A. Miyawaki, J. Hofkens, *J. Am. Chem. Soc.* **2007**, *129*, 16132.
63. Y. Takagi, M. Morimoto, R. Kashihara, S. Fujinami, S. Ito, H. Miayasaka, M. Irie, *Tetrahedron* **2017**, *73*, 4918.
64. R. Kashihara, M. Morimoto, S. Ito, H. Miyasaka, M. Irie, *J. Am. Chem. Soc.* **2017**, *139*, 16498.
65. T. Sumi, T. Kaburaki, M. Morimoto, K. Une, H. Sotome, S. Ito, H. Miyasaka, M. Irie, *Org. Lett.* **2015**, *17*, 4802.
66. T. Fukaminato, T. Hirose, T. Doi, M. Hazama, K. Matsuda, M. Irie, *J. Am. Chem. Soc.* **2014**, *136*, 17145.
67. S. Fredrich, R. Göstl, M. Herder, L. Grubert, S. Hecht, *Angew. Chem. Int. Ed.* **2016**, *55*, 1208.
68. F. Wondrazek, A. Seilmeier, W. Kaiser, *Chem. Phys. Lett.* **1984**, *104*, 121.
69. S. Kinoshita, N. Nishi, A. Saitoh, T. Kushida, *J. Phys. Soc. Jpn.* **1987**, *56*, 4162.
70. K. Mizuno, A. Matsui, G. J. Sloan, *J. Phys. Soc. Jpn.* **1984**, *53*, 2799.
71. F. Urbach, *Phys. Rev.* **1953**, *92*, 1324.
72. J. B. Birks, *Photopysics of Aromatic Molecules*; John Wiley & Sons Ltd: London, **1970**.
73. B. Roubinet, M. L. Bossi, P. Alt, M. Leutenegger, H. Shojaei, S. Schnorrenberg, S. Nizamov, M. Irie, V. N. Belov, S. W. Hell. S. *Angew. Chem. Int. Ed.* **2016**, *55*, 15429.
74. O. Nevskyi, D. Sysoiev, A. Oppermann, T. Huhn, D. Wöll, D. *Angew. Chem. Int. Ed.* **2016**, *55*, 12698.
75. Y. Arai, S. Ito, H. Fujita, Y. Yoneda, T. Kaji, S. Takei, R. Kashihara, M. Morimoto, M. Irie, H. Miyasaka, *Chem. Commun.* **2017**, *53*, 4066.
76. B. Roubinet, M. Weber, H. Shojaei, M. Bates, M. L. Bossi, V. N. Belov, M. Irie, S. W. Hell. *J. Am. Chem. Soc.* **2017**, *139*, 6611.
77. Y. Shoji, A. Yagi, M. Horiuchi, M. Morimoto, M. Irie, *Isr. J. Chem*. **2013**, *53*, 303.

78. F. Balzarotti, Y. Eilers, K. C. Gwosch, A. H. Gynnå, V. Westphal, F. D. Stefani, J. Elf, S. W. Hell, *Science* **2017**, *355*, 606.

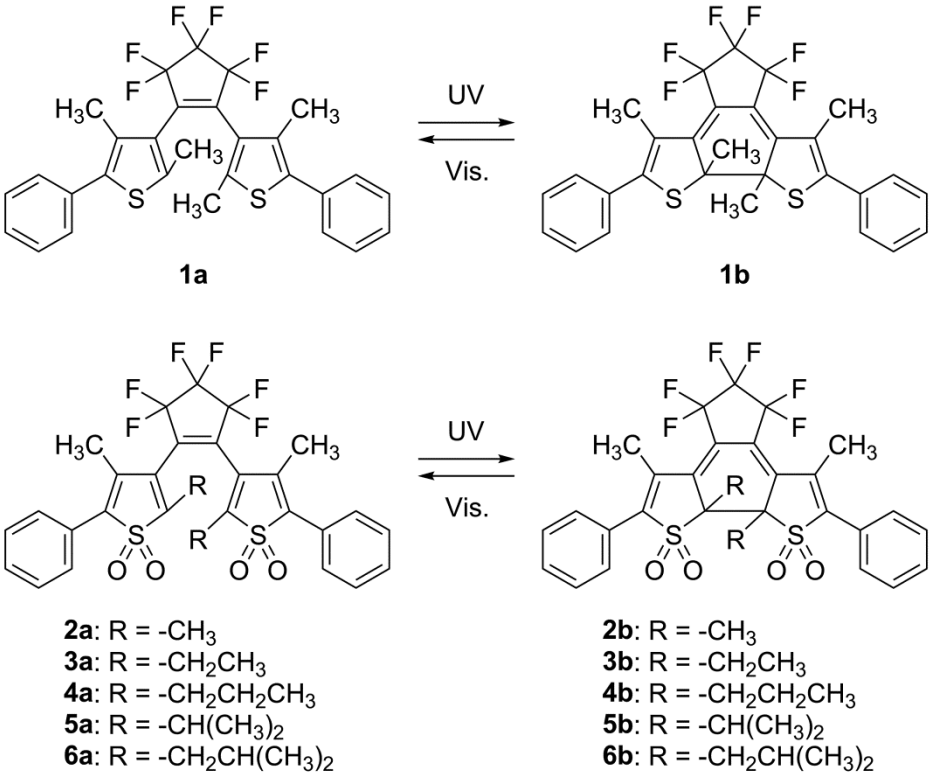

Scheme 1. Photoisomerization of diarylethenes **1**–**6**.

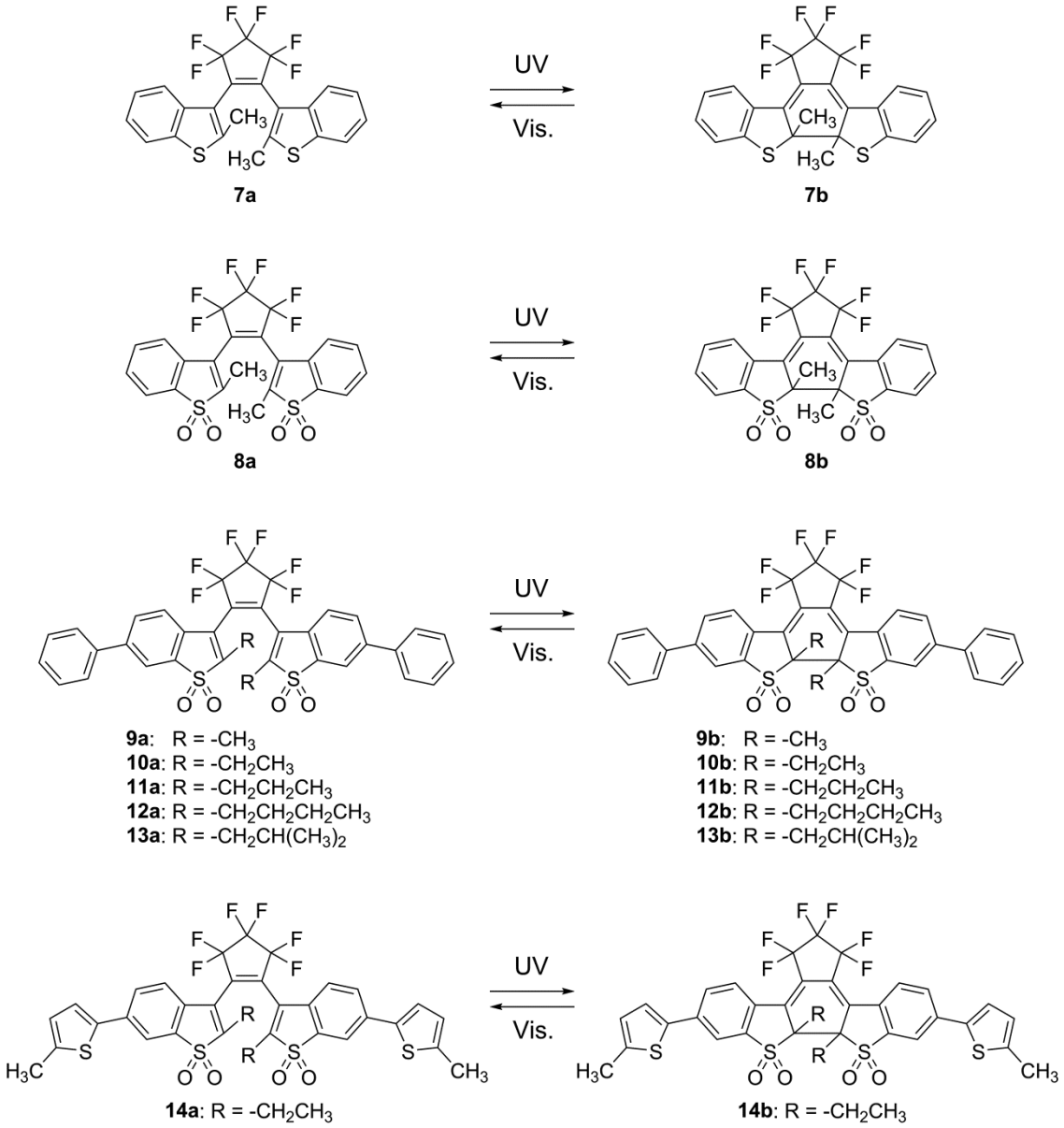

Scheme 2. Photoisomerization of diarylethenes **7**–**14**.

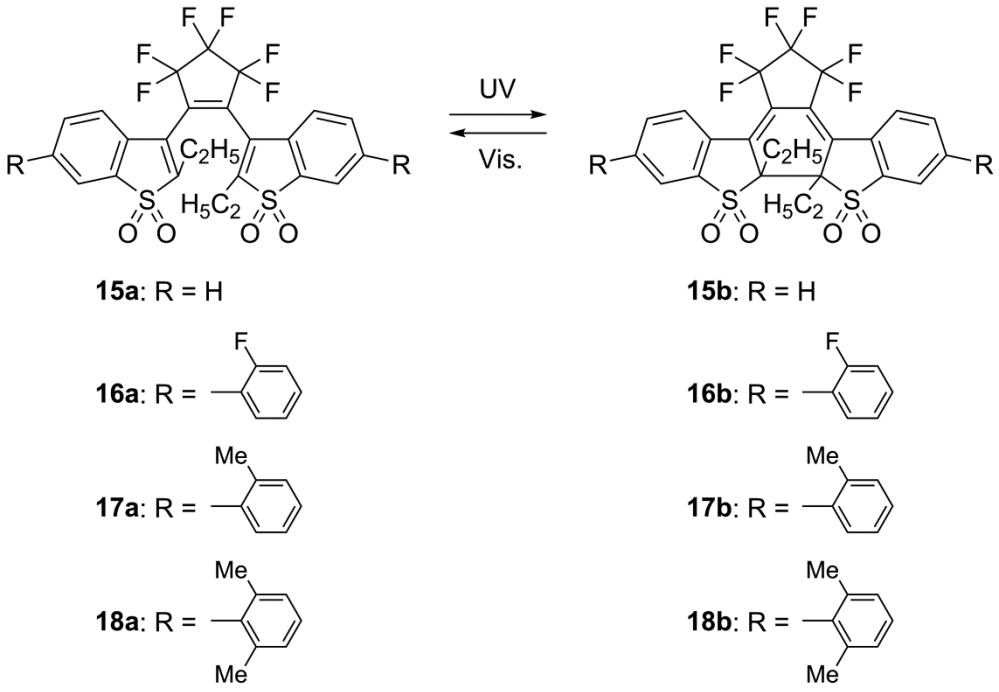

Scheme 3. Photoisomerization of diarylethenes **15**–**18**.

Table 1. Photophysical and photochemical properties of **2**–**6** in 1,4-dioxane. λ_{max}: absorption maximum, ε: molar absorption coefficient, Φ_{oc}: cyclization quantum yield under irradiation with 313 nm light, Φ_{co}: cycloreversion quantum yield under irradiation with 450 nm light, Φ_f: fluorescence quantum yield under irradiation at the absorption maximum.

	Open-ring isomer, **a**		Closed-ring isomer, **b**		
	λ_{max} / nm (ε / 10^4 M^{-1} cm^{-1})	Φ_{oc}	λ_{max} / nm (ε / 10^4 M^{-1} cm^{-1})	Φ_{co}	Φ_f
2	296 (0.79)	0.14	424 (2.4)	3.5×10^{-5}	0.07
3	297 (0.79)	0.09	433 (2.2)	3.8×10^{-5}	0.42
4	298 (0.80)	0.10	434 (2.1)	7.1×10^{-5}	0.42
5	301 (0.79)	0.21	427 (1.8)	2.6×10^{-5}	0.42
6	299 (0.83)	0.12	438 (2.1)	2.1×10^{-3}	0.50

Table 2. Photophysical and photochemical properties of **8**–**14**. λ_{max}: absorption maximum, ε: molar absorption coefficient, Φ_{oc}: cyclization quantum yield, Φ_{co}: cycloreversion quantum yield, Φ_f: fluorescence quantum yield. Ethyl acetate and 1,4-dioxane were used as solvents for **8** and **9**–**14**, respectively.

	Open-ring isomer, **a**		Closed-ring isomer, **b**		
	λ_{max} / nm (ε / 10^4 $M^{-1}cm^{-1}$)	Φ_{oc}	λ_{max} / nm (ε / 10^4 $M^{-1}cm^{-1}$)	Φ_{co}	Φ_f
8	276 (0.37), 308 (0.41)	0.22 [a]	398 (2.10)	0.061 [d]	0.011
9	296 (1.8), 335 (1.4)	0.61 [b,c,g]	443 (5.1)	1.2×10^{-3} [e,g]	0.64
10	298 (1.9), 336 (1.5)	0.62 [b,c,g]	456 (4.6)	5.9×10^{-4} [e,g]	0.87
11	297 (2.0), 336 (1.6)	0.58 [c,g]	456 (4.5)	9.0×10^{-4} [e,g]	0.89
12	298 (2.0), 336 (1.6)	0.56 [c,g]	456 (4.5)	1.2×10^{-3} [e,g]	0.85
13	300 (1.6), 336 (1.4)	0.62 [b]	460 (3.7)	1.1×10^{-2} [e]	0.80
14	330 (2.4), 374 (2.5)	0.23 [c,g]	506 (5.8)	$< 1.0 \times 10^{-5}$ [e,f,g]	0.78

[a] Under irradiation with 312 nm light.
[b] Under irradiation with 313 nm light.
[c] Under irradiation with 330 nm light.
[d] Under irradiation at λ_{max} of closed-ring isomer.
[e] Under irradiation with 450 nm light.
[f] Under irradiation with 488 nm light.
[g] Re-examined using a photoreaction quantum yield measuring system (Shimadzu, QYM-01) with a corrected power meter.

Table 3. Photophysical photochemical properties of **15–18** in 1,4-dioxane. λ_{max}: absorption maximum, ε: absorption coefficient, Φ_{oc}: cyclization quantum yield, Φ_{co}: cycloreversion quantum yield, Φ_f: fluorescence quantum yield, τ_f: fluorescence lifetime. ω: averaged dihedral angle between the phenyl ring and the oxidized benzothiophene observed by X-ray crystallographic analysis.

	Open-ring isomer, **a**		Closed-ring isomer, **b**				ω / °
	λ_{max} / nm (ε / 10^4 $M^{-1}cm^{-1}$)	Φ_{oc}	λ_{max} / nm (ε / 10^4 M^{-1} cm^{-1})	Φ_{co}	Φ_f	τ_f / ns	
15	275 (0.52), 310 (0.52)	0.28 [a]	414 (1.8)	0.18 [c]	0.22	1.2	–
16	293 (1.7), 328 (1.4)	0.58 [b]	445 (4.2)	2.8×10^{-3} [d]	0.79	3.0	35.9
17	289 (1.2), 326 (1.0)	0.63 [b]	441 (3.7)	3.2×10^{-3} [d]	0.84	3.1	61.0
18	285 (0.97), 320 (0.82)	0.59 [b]	430 (3.5)	1.8×10^{-2} [d]	0.79	3.2	65.7

[a] Under irradiation with 313 nm light.
[b] Under irradiation with 330 nm light.
[c] Under irradiation with 405 nm light.
[d] Under irradiation with 450 nm light.

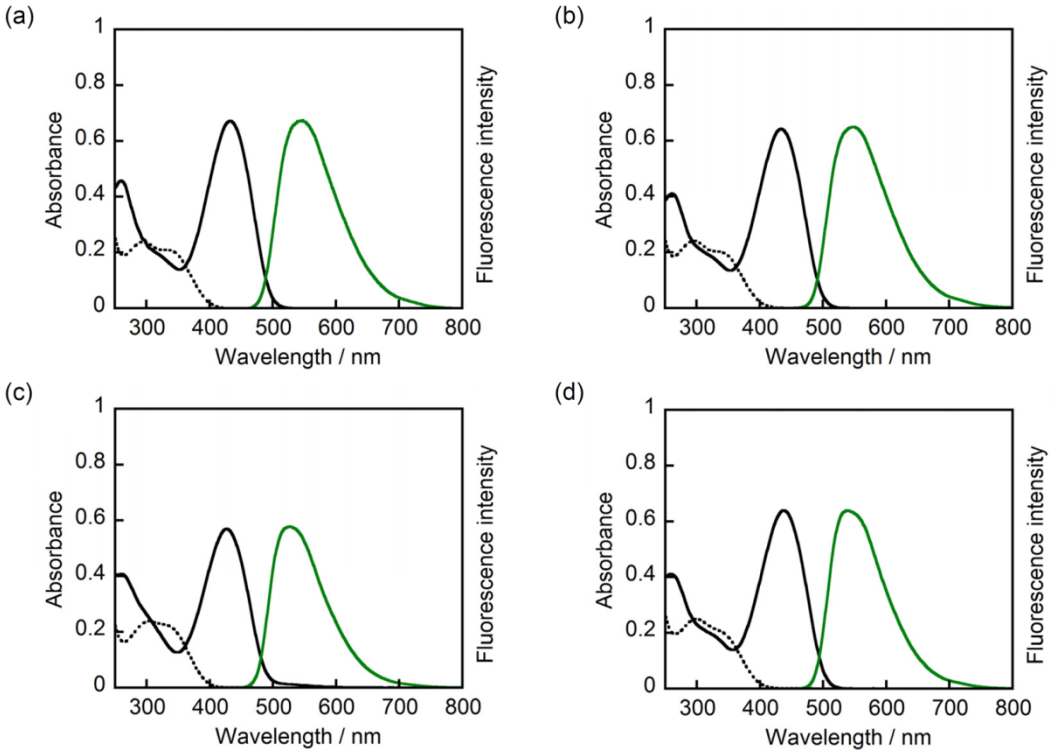

Figure 1. Absorption and fluorescence spectra of **3** (a), **4** (b), **5** (c), and **6** (d) in 1,4-dioxane (3.0×10^{-5} M). Black dashed lines: absorption spectra of open-ring isomers **3a**–**6a**, black solid lines: absorption spectra of closed-ring isomers **3b**–**6b**, green solid lines: fluorescence spectra (uncorrected) of closed-ring isomers **3b**–**6b**.

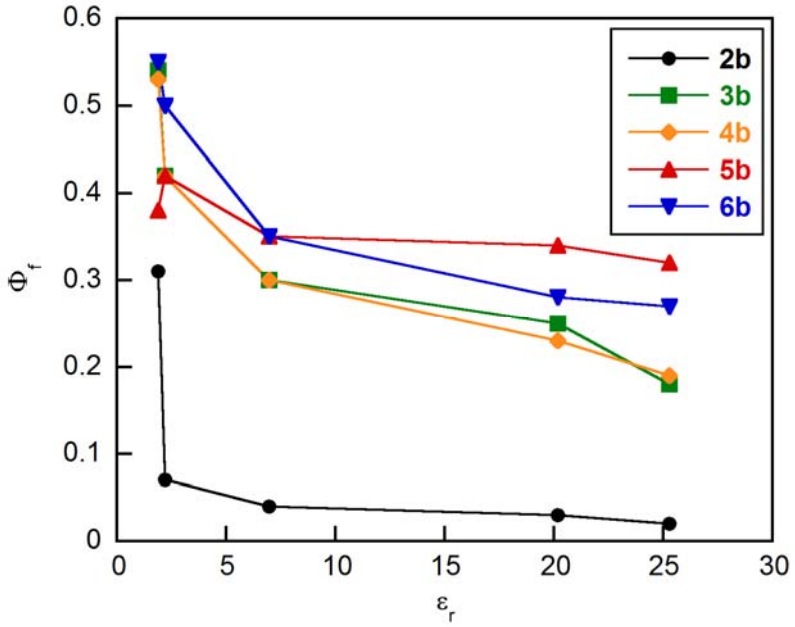

Figure 2. Relationship between fluorescence quantum yields (Φ_f) of closed-ring isomers **2b**–**6b** and the relative dielectric constants (ε_r) of the solvents. The solvents used are *n*-hexane (ε_r = 1.89), 1,4-dioxane (ε_r = 2.22), 2-methyltetrahydrofuran (ε_r = 6.97), 2-propanol (ε_r = 20.2), and ethanol (ε_r = 25.3).

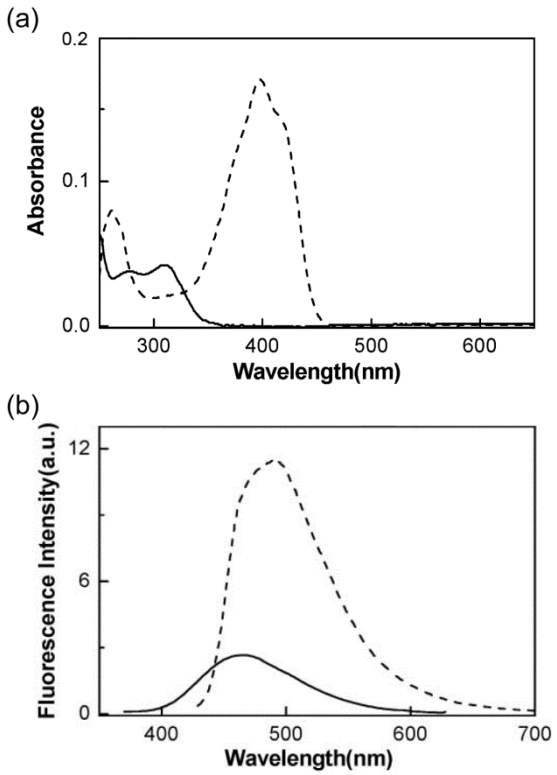

Figure 3. (a) Absorption spectra of **8a** (solid line) and **8b** (dashed line) in ethyl acetate (1.0×10^{-5} M). (b) Fluorescence spectra of **8a** (solid line) and **8b** (dashed line) in ethyl acetate (1.0×10^{-5} M) under photo-excitation at the absorption maxima. Reproduced from ref. 51 with permission from The Royal Society of Chemistry.

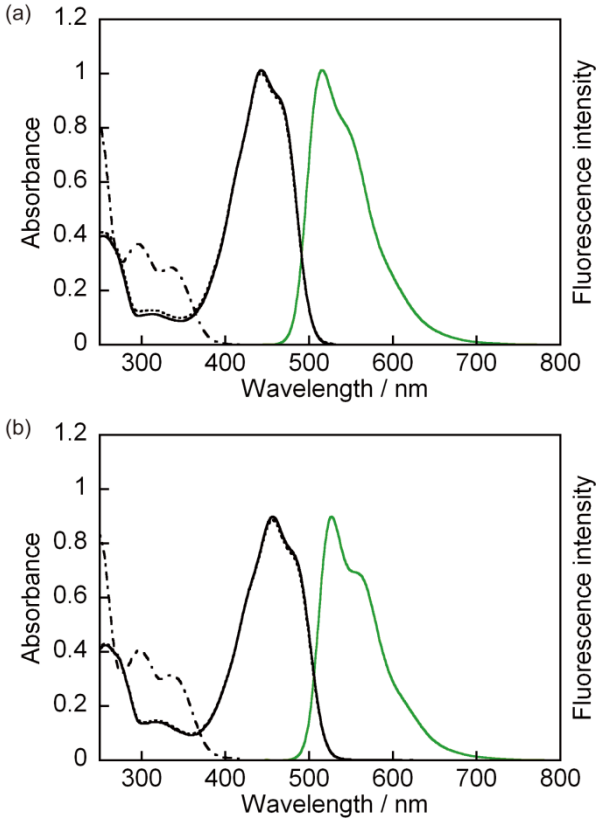

Figure 4. Absorption spectra of open-ring isomers (black dot-dashed line), closed-ring isomers (black solid line) and photostationary states under irradiation with 330 nm light (black dotted line) and fluorescence spectra of closed-ring isomers under irradiation with 450 nm light (green solid line, uncorrected) in 1,4-dioxane (2.0×10^{-5} M). (a) **9**, (b) **12**. Reproduced from ref. 60 with permission of The Royal Society of Chemistry (RSC) on behalf of the Centre National de la Recherche Scientifique (CNRS) and the RSC.

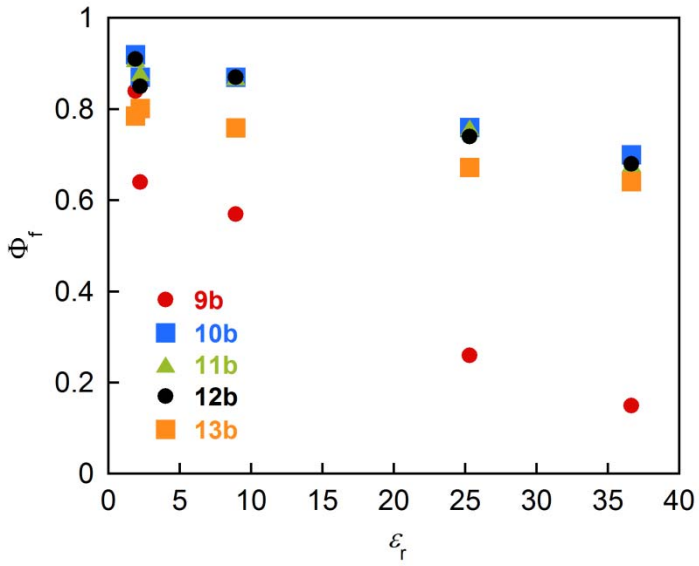

Figure 5. Relationship between fluorescence quantum yields (Φ_f) and relative dielectric constants of the solvents (ε_r, hexane: 1.89, 1,4-dioxane: 2.22, dichloromethane: 8.93, ethanol: 25.3, acetonitrile: 36.64). Red circles: **9b**, blue squares: **10b**, green triangles: **11b**, black circles: **12b**, orange squares: **13b**. Adapted from ref. 60 with permission of The Royal Society of Chemistry (RSC) on behalf of the Centre National de la Recherche Scientifique (CNRS) and the RSC.

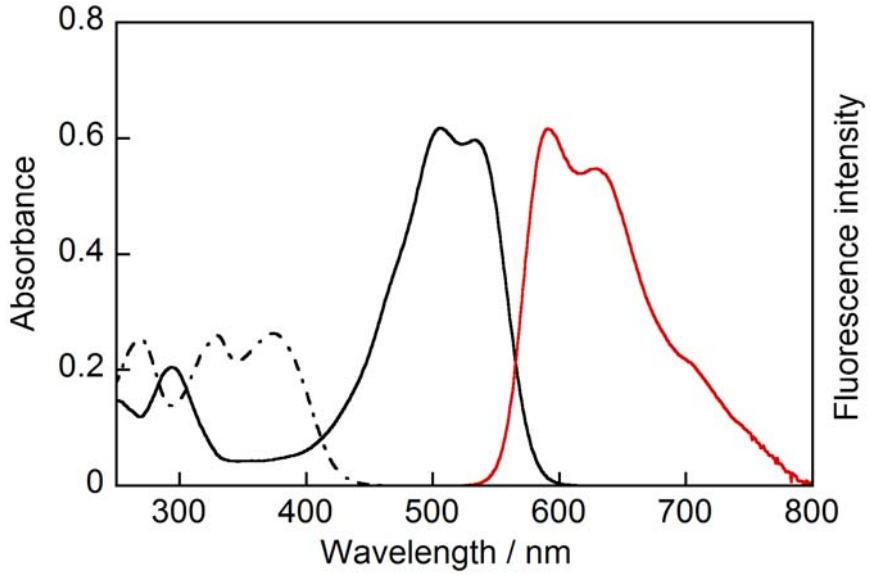

Figure 6. Absorption spectra of **14a** (black dot-dashed line), **14b** (black solid line) and photostationary state under irradiation with 365 nm light in 1,4-dioxane (1.0×10^{-5} M) and fluorescence spectrum of **14b** (red solid line) under excitation with 532 nm light. The photostationary spectrum overlaps with the spectrum of **14b** due to 100% photoconversion. Reprinted with permission from ref. 47. Copyright 2011 American Chemical Society.

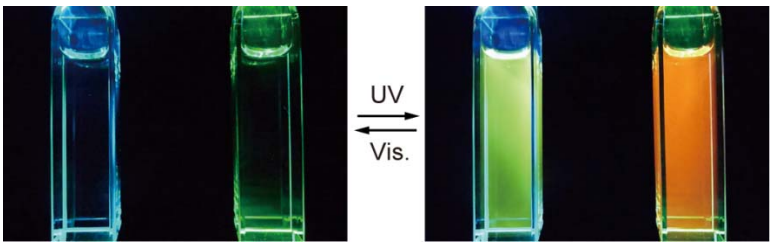

Figure 7. Photographs of 1,4-dioxane solutions containing **10** and **14** before and after irradiation with 365 nm light under excitation with 488 nm blue light (left-side solution containing **10**) and 532 nm green light (right-side solution containing **14**). Reprinted with permission from ref. 47. Copyright 2011 American Chemical Society.

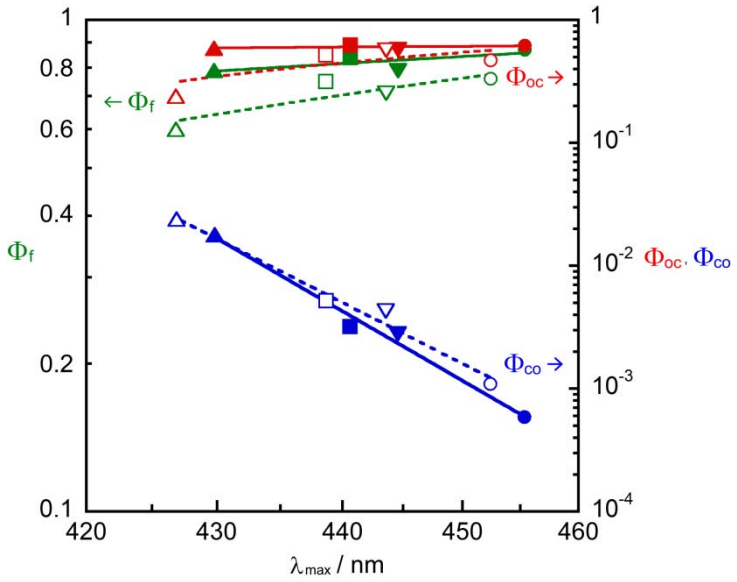

Figure 8. Correlation between absorption maxima of the closed-ring isomers (λ_{max}) and quantum yields of cycloreversion (Φ_{co}, blue) and cyclization (Φ_{oc}, red) of **10** (●,○), **16** (▼,∇), **17** (■,□), and **18** (▲,△) in 1,4-dioxane (closed marks) and ethanol (open marks). Fluorescence quantum yields (Φ_f, green) of the closed-ring isomers of **10** (●,○), **16** (▼,∇), **17** (■,□), and **18** (▲,△) in 1,4-dioxane (closed marks) and ethanol (open marks) were also plotted. Reprinted from ref. 63, Copyright 2017, with permission from Elsevier.

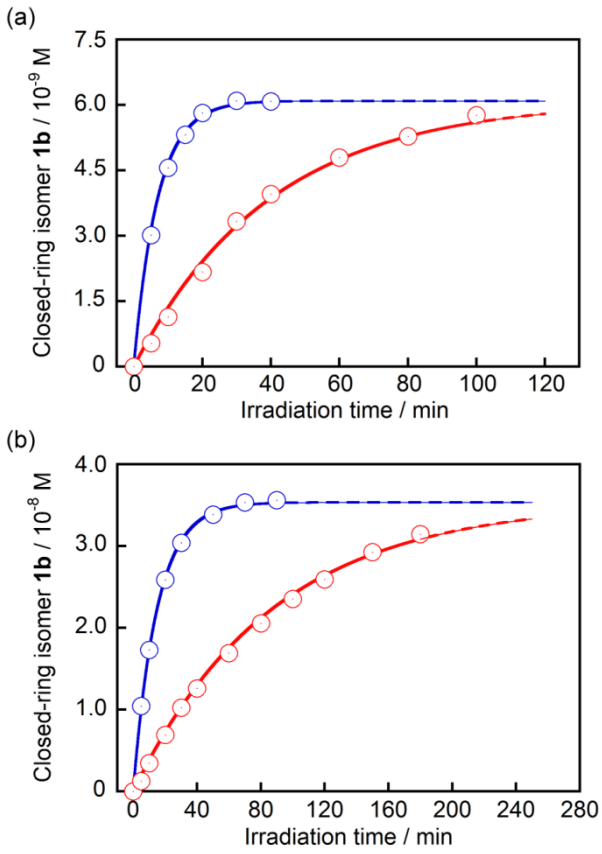

Figure 9. Formations of closed-ring isomer **10b** from pure **10a** (1.0×10^{-5} M) in *n*-hexane (a) and CCl_4 (b) upon irradiation with monochromatic 450 nm light. The two formation curves were measured by changing the light intensity, 100% (blue) and 25% (red), respectively. Solid lines were simulated by using eq. (3). Reprinted with permission from ref. 64. Copyright 2017 American Chemical Society.

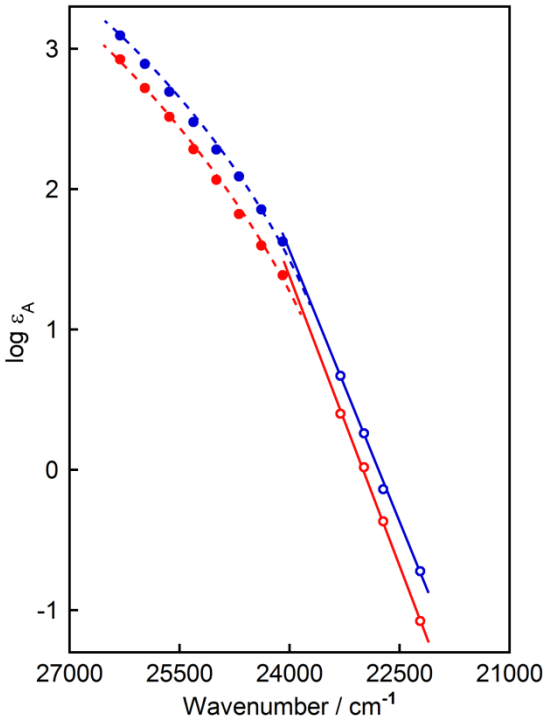

Figure 10. Logarithmic plot of molar absorption coefficients of **10a** (ε_A) in *n*-hexane (red) and CCl_4 (blue) obtained from absorption spectra of **10a** (closed circles) and fluorescence intensities of **10b** in the photostationary states under irradiation with monochromatic visible light (open circles). Reprinted with permission from ref. 64. Copyright 2017 American Chemical Society.

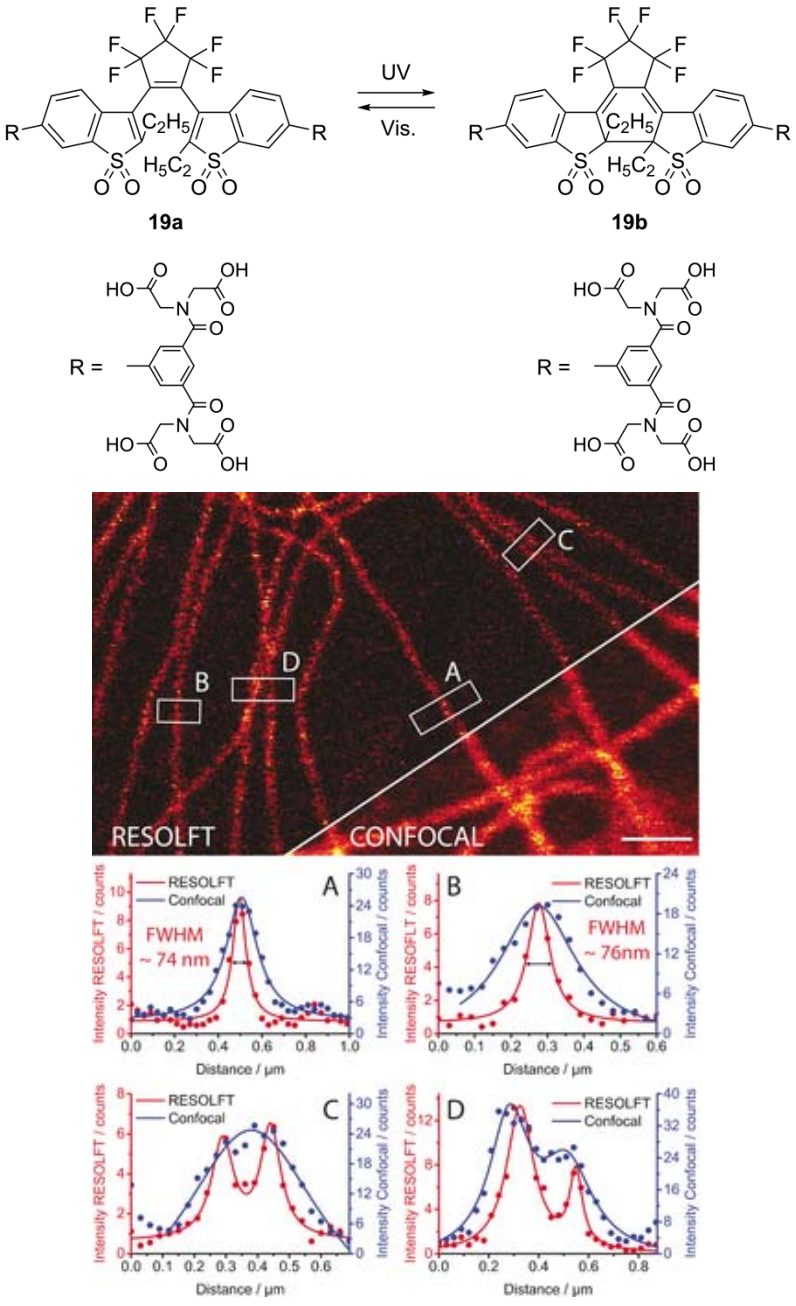

Figure 11. RESOLFT images of the whole fixed Vero cells immunostained with primary antibodies against α-Tubulin and with the diarylethene **19** attached to the secondary antibodies. The RESOLFT images were recorded before confocal images. Scale bar: 1 µm. The line profiles A–D (averaged over ten adjacent lines) display the regions indicated in the RESOLFT image. The data (dots) was fitted with a Lorentzian function (solid line) for the RESOLFT (red) and the confocal (blue) image. Adapted with permission from ref. 73. Copyright 2016 Wiley-VCH Verlag GmbH & Co. KGaA, Weinheim.

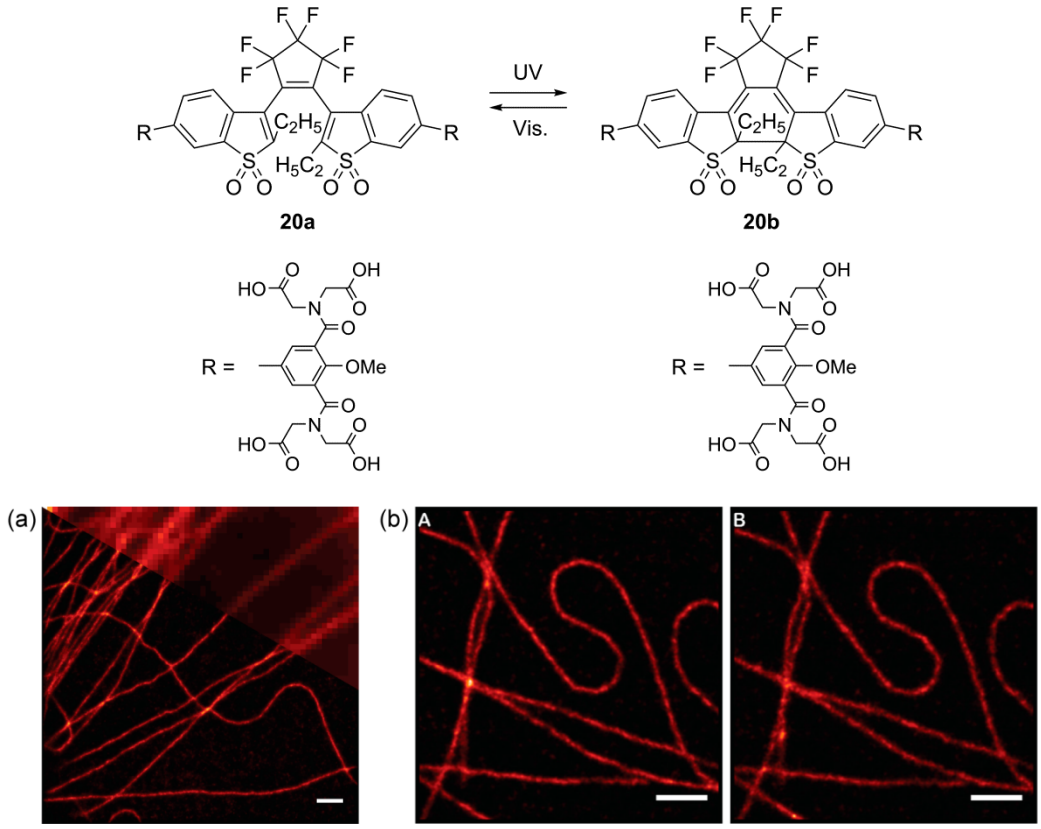

Figure 12. (a) Super-resolution image (STORM) *without activation light* of Vero cells immunostained with a primary antibody against tubulin and a secondary antibody labeled with compound **20** (DOL = 3.5). Mounting medium used was PBS (pH 7.4). A wide-field image, generated as the sum of all frames, is overlaid on the upper part of the image. Scale bar, 1 μm; image frames, 200 000; localizations, ~1 × 10^6. (b) Super-resolution images (STORM) of Vero cells labeled with compound **20** without (A) and with (B) UV activation. Mounting medium used was PBS (pH 7.4). Scale bar, 1 μm; image frames (raw), 50 000 each case; localizations, ~ 90 000 each. Reprinted with permission from ref. 76. Copyright 2017 American Chemical Society.

Biography

Masahiro Irie received his B.S. and M.S. degrees from Kyoto University and his Ph.D. degree in radiation chemistry from Osaka University. In 1968, he joined the Faculty of Engineering, Hokkaido University and started his research on photochemistry. He was the faculty member at Osaka University, Kyushu University and Rikkyo University. He has been conducting research on molecular photoswitches for the last 40 years. In the middle of the 1980s he discovered thermally irreversible and fatigue resistant photochromic diarylethenes. His current interest focuses on the development of light-driven molecular-crystal actuators and turn-on mode fluorescent diarylethenes for super-resolution fluorescence microscopies.